PNAS RESEARCH ARTICLE | PLANT BIOLOGY OPEN ACCESS

Divergent evolution of extreme production of variant plant monounsaturated fatty acids

Lu Gan[a,b,c,1,2], Kiyoul Park[a,b,c,1], Jin Chai[d], Evan M. Updike[a,b,c], Hyojin Kim[a,b,c], Adam Voshall[b,e], Sairam Behera[b,f], Xiao-Hong Yu[g], Yuanheng Cai[g], Chunyu Zhang[h], Mark A. Wilson[c], Jeffrey P. Mower[b,i], Etsuko N. Moriyama[b,e], Chi Zhang[b,e], Sireewan Kaewsuwan[j], Qun Liu[d], John Shanklin[d], and Edgar B. Cahoon[a,b,c,2]

Edited by Chris Somerville, University of California, Berkeley, CA; received January 20, 2022; accepted June 12, 2022

Metabolic extremes provide opportunities to understand enzymatic and metabolic plasticity and biotechnological tools for novel biomaterial production. We discovered that seed oils of many *Thunbergia* species contain up to 92% of the unusual monounsaturated petroselinic acid (18:1Δ6), one of the highest reported levels for a single fatty acid in plants. Supporting the biosynthetic origin of petroselinic acid, we identified a Δ6-stearoyl-acyl carrier protein (18:0-ACP) desaturase from *Thunbergia laurifolia*, closely related to a previously identified Δ6-palmitoyl-ACP desaturase that produces sapienic acid (16:1Δ6)-rich oils in *Thunbergia alata* seeds. Guided by a *T. laurifolia* desaturase crystal structure obtained in this study, enzyme mutagenesis identified key amino acids for functional divergence of Δ6 desaturases from the archetypal Δ9-18:0-ACP desaturase and mutations that result in nonnative enzyme regiospecificity. Furthermore, we demonstrate the utility of the *T. laurifolia* desaturase for the production of unusual monounsaturated fatty acids in engineered plant and bacterial hosts. Through stepwise metabolic engineering, we provide evidence that divergent evolution of extreme petroselinic acid and sapienic acid production arises from biosynthetic and metabolic functional specialization and enhanced expression of specific enzymes to accommodate metabolism of atypical substrates.

fatty acid | vegetable oil | chemical diversity | desaturase | biotechnology

Seed oils are characterized by diverse fatty acid (FA) structures (1–3). Many of these deviate from typical C16 (e.g., palmitic acid, 16:0) and C18 (e.g., oleic acid, 18:1Δ9*cis*) FA that occur widely in seed oils, including major commercial vegetable oils. Structurally variant FAs, often referred to as "unusual" FAs, can have chain lengths other than 16 or 18 carbon atoms, double bonds in nontypical positions or *cis-trans* configurations, or carbon-chain modifications, such as hydroxyl or epoxy groups (4). The study of unusual FA biochemistry has increased understanding of enzyme structural determinants of substrate binding and reaction outcomes (4). These studies have also revealed how variations in biosynthetic and metabolic pathways allow for high levels of unusual FA biosynthesis and accumulation and have also facilitated research on the evolution of biochemical diversity in plants. Unusual FAs can occur in selected species or arise throughout a genus or family, and their accumulation may be associated with compensatory mutations in enzymes beyond the initial biosynthetic enzyme (5). Moreover, genes for unusual FA biosynthesis and metabolism can be useful for biotechnological research in plants and microbes to develop vegetable oils with enhanced nutritional or industrial value (6).

In a variety of taxa, metabolic variations result in "extreme" unusual FA accumulation to ≥90% of seed oil, which can account for ≤50% of seed weight (2). Examples of extreme unusual FA production include medium chain-length FAs (C8–C14) in seeds of *Cuphea* species and ricinoleic acid, a hydroxylated C18 monounsaturated FA in castor seeds (*Ricinus communis*) (7, 8). Studies of FA metabolism in *Cuphea* have uncovered structurally variant FatB acyl-acyl carrier protein (ACP) thioesterases and acyltransferases associated with the biosynthesis and accumulation of medium chain-length FAs. These variant thioesterases have provided primary sequences for uncovering information about amino acid residues that control their substrate recognition properties (9–11). Studies of FA metabolism in castor seeds led to the discovery that structural variations in *FAD2* genes for Δ12-oleic acid desaturases can lead to variant FA modifications, including insertion of hydroxyl and epoxy groups, triple bonds, and conjugated double bonds (12–14). FA biosynthetic and metabolic genes associated with these pathways have also been used to develop new oil functionalities in existing oilseed crops.

Studies of unusual monounsaturated FAs have provided a wealth of biochemical information and biotechnological utility (15). Oleic acid, the most widely occurring

Significance

The dietary and oleochemical value of vegetable oils is determined by their component fatty acids. Double bonds or "unsaturation" in fatty acids are critical for vegetable oil functionality. Seeds containing vegetable oils with extremely high levels of a single fatty acid have provided insights into enzyme-substrate recognition and metabolic plasticity and genes for biotechnological improvement of oilseeds. We report the discovery of species with seed oils containing >90% of an unusual monounsaturated fatty acid. We identified the variant enzyme that produces this fatty acid and elucidated its three-dimensional structure. We used this information to develop enzymes that produce nonnaturally occurring monounsaturated fatty acids and sourced genes from these species to engineer oilseeds and bacteria for modified fatty acid compositions.

Author contributions: L.G., K.P., E.M.U., H.K., J.P.M., Chi Zhang, Q.L., J.S., and E.B.C. designed research; L.G., K.P., J.C., E.M.U., H.K., A.V., S.B., X.-H.Y., Y.C., M.A.W., J.P.M., E.N.M., Chi Zhang, S.K., Q.L., and E.B.C. performed research; Chunyu Zhang and S.K. contributed new reagents/analytic tools; L.G., K.P., J.C., E.M.U., H.K., Chunyu Zhang, Chi Zhang, S.K., Q.L., J.S., and E.B.C. analyzed data; and L.G., K.P., H.K., J.P.M., Q.L., J.S., and E.B.C. wrote the paper.

The authors declare no competing interest.

This article is a PNAS Direct Submission.

[1]L.G. and K.P. contributed equally to this work.

[2]To whom correspondence may be addressed. Email: lgan3@unl.edu or ecahoon2@unl.edu.

This article contains supporting information online at http://www.pnas.org/lookup/suppl/doi:10.1073/pnas.2201160119/-/DCSupplemental.

Published July 22, 2022.

monounsaturated FA in plants, is synthesized by the soluble Δ9-stearoyl-ACP desaturase (16). Structural variants of this enzyme result in a number of unusual FAs, including palmitoleic acid (16:1Δ9), sapienic acid (16:1Δ6), and petroselinic acid (18:1Δ6) (15). Studies of variant acyl-ACP desaturases in combination with three-dimensional (3D) structural data (17, 18) have revealed amino acid residues that control FA chain length- and regio-specificities of this enzyme class (19). This information has facilitated biotechnological development of oilseeds with high levels of unusual monounsaturated FAs using rationally designed acyl-ACP desaturases (20). In the case of petroselinic acid, a biosynthetic pathway has been deduced that involves not only a variant Δ4-16:0-ACP desaturase but also a coevolved variant β-ketoacyl-ACP synthase I and acyl-ACP thioesterase that together generate petroselinic acid at ≤85% of the total FAs of Apiaceae and Araliaceae seeds (21–24). This highlights that unusual FA biosynthesis can result from the initial evolution of a specialized biosynthetic enzyme, followed by evolution of additional enzymes that facilitate unusual FA production and accumulation.

As part of our larger efforts to characterize the evolution of unusual FA biosynthesis in plants, we examined the FA composition of seeds in diverse *Thunbergia* species. It has been previously shown that *Thunbergia alata* seeds accumulate sapienic acid (16:1Δ6*cis*) to ∼85% of total FAs via the activity of a Δ6-16:0-ACP desaturase (25, 26). As reported here, we discovered that seeds of several *Thunbergia* species accumulate petroselinic acid instead of sapienic acid. In these seeds, petroselinic acid accumulates >90% of total FAs, which is among the highest naturally occurring levels of monounsaturated FA in plant seed oils. We provide biochemical, structural, and genetic evidence to explain the divergent evolution of increased sapienic and petroselinic acid production in *Thunbergia*. Furthermore, we show that the petroselinic acid biosynthetic pathway in *Thunbergia* is distinct from that in Apiaceae and Araliaceae (21) and can guide biotechnological production of unusual monounsaturated FAs in engineered crops and microbes.

Results

Identification of Petroselinic Acid as the Predominant FA in *Thunbergia* Seeds. Studies were initiated to determine if sapienic acid (16:1Δ6)-rich seed oil reported in *T. alata* occurs widely in the *Thunbergia* genus. Using gas chromatography-flame ionization detection (GC-FID), we unexpectedly found a near absence of 16:1Δ6 FAs in *Thunbergia laurifolia* seeds (Fig. 1 *A* and *B*). Instead, these seeds are enriched in octadecenoic acid (18:1), which accounts for >90% of seed total FAs (Fig. 1*B*). Analysis of the 18:1 double-bond position by mass spectrometry (MS) revealed almost entirely the Δ6 isomer, indicating petroselinic acid (18:1Δ6) is the predominant FA in *T. laurifolia* seeds (Fig. 1*C*). By comparison, the "typical" 18:1 isomer oleic acid (18:1Δ9) comprised <1.5% of seed FAs (Fig. 1*B*). Petroselinic acid was found to account for ∼92% of triacylglycerol (TAG), the primary lipid of *T. laurifolia* seeds, but <20% of the FAs of phosphatidylcholine (PC), the major membrane phospholipid of these seeds (Fig. 1*D*). A survey of commercially available *Thunbergia* seeds indicated petroselinic acid also comprises up to 92% of the total FAs and TAG of *Thunbergia grandiflora*, *Thunbergia coccinea*, *Thunbergia natalensis*, and *Thunbergia lutea* seeds (Fig. 1*E* and *SI Appendix*, Fig. S1*A*). Similar to *T. alata* seeds, *Thunbergia fragrans* seeds were found to contain 16:1Δ6 at ∼80% of total FAs, as confirmed by mass spectrometry (Fig. 1*E* and *SI Appendix*, Fig. S2). Total oil ranged from ∼16% of total seed weight in *T. laurifolia* and *T. coccinea* seeds to ∼45% in *T. lutea* seeds (*SI Appendix*, Fig. S1*B*).

Identification of Variant acyl-ACP Desaturases in *T. laurifolia* Seeds. We hypothesized that petroselinic acid in *Thunbergia* seeds is produced by a Δ6 desaturase that is most active with 18:0-ACP and is distinct from the Δ6-16:0-ACP desaturase previously identified in *T. alata* (25). Acyl-ACP desaturase cDNAs were isolated from developing *T. laurifolia* seeds through PCR with degenerate oligonucleotides designed from conserved amino acid sequences in functionally diverse acyl-ACP desaturases (*SI Appendix*, Fig. S3). Full-length cDNAs for two acyl-ACP desaturases sharing 98% amino acid identity, designated DES6-1 and DES6-2, were isolated. The amino acid sequences of these desaturases are most closely related to the *T. alata* Δ6-16:0-ACP desaturase (∼86% identity) (25), but share ≤70% identity with other known acyl-ACP desaturases, including *T. alata* Δ9-18:0-ACP desaturases (27). Phylogenetic analyses indicated no close relationship between the primary structures of the *T. laurifolia* acyl-ACP desaturases and coriander (*Coriandrum sativum*) and English ivy (*Hedera helix*) Δ4-16:0-ACP desaturases associated with petroselinic acid biosynthesis (22, 27, 28) (Fig. 2*A*). Broader phylogenetic analysis indicated evolutionary relationship between the *Thunbergia aurifolia* and *T. alata* Δ6 and Δ9 desaturases, consistent with a recent sequential evolution of the *T. laurifolia* and *T. alata* Δ6 desaturases from the canonical Δ9-18:0-ACP desaturase within the *Thunbergia* genus (*SI Appendix*, Fig. S4). However, a more distantly related *T. laurifolia* Δ9-18:0-ACP desaturase was identified from sequences in a *T. laurifolia* seed transcriptome (Fig. 2*A* and *SI Appendix*, Fig. S4). Amino acid sequence comparisons also revealed conserved amino acid differences between the *T. laurifolia* desaturases and other acyl-ACP desaturases (Fig. 2*B*).

We compared activities of *T. laurifolia* acyl-ACP desaturase (DES6-1) and *T. alata* Δ6-16:0-ACP desaturase using purified *Escherichia coli*-expressed mature polypeptides (lacking the N-terminal plastid transit peptide sequence) (Fig. 2 *C* and *D* and *SI Appendix*, Fig. S5 *A* and *B*). The *T. laurifolia* acyl-ACP desaturase was ∼20-fold more active with 18:0-ACP than with 16:0-ACP (Fig. 2*C*). This enzyme generated only a Δ6 monounsaturated product with 18:0-ACP, as determined by argentation thin-layer chromatography (TLC) mobility and confirmed by GC-MS of dimethyl disulfide derivatives of assay products with 17:0-ACP (Fig. 2*E*). The enzyme was found to have mixed Δ6/Δ9 functionality with 16:0-ACP (Fig. 2*C*). These findings were the converse of the *T. alata* Δ6 desaturase activity, which was approximately six-fold more active with 16:0-ACP than with 18:0-ACP (Fig. 2*D*). The *T. alata* enzyme functioned exclusively as a Δ6 desaturase with 16:0-ACP, but had mixed Δ6/Δ9 regiospecificity with 18:0-ACP (Fig. 2*D*). These results demonstrated that functionally distinct *T. laurifolia* and *T. alata* Δ6 desaturases dictate different monounsaturated FA compositions of seed oils in these species.

Structure-Guided Study of *T. laurifolia* acyl-ACP Desaturase Regiospecificity. The structural basis for divergent evolution of *T. laurifolia* and *T. alata* Δ6 desaturases from archetypal Δ9-18:0-ACP desaturases was explored. We assessed activities of *T. alata* and *T. laurifolia* desaturase mutants, targeting: 1) amino acid differences in regions known to affect substrate specificity (19) and 2) conserved amino acid differences between these enzymes and Δ9-18:0-ACP desaturases (Fig. 2*B*). We used purified recombinant enzymes and measured relative differences in

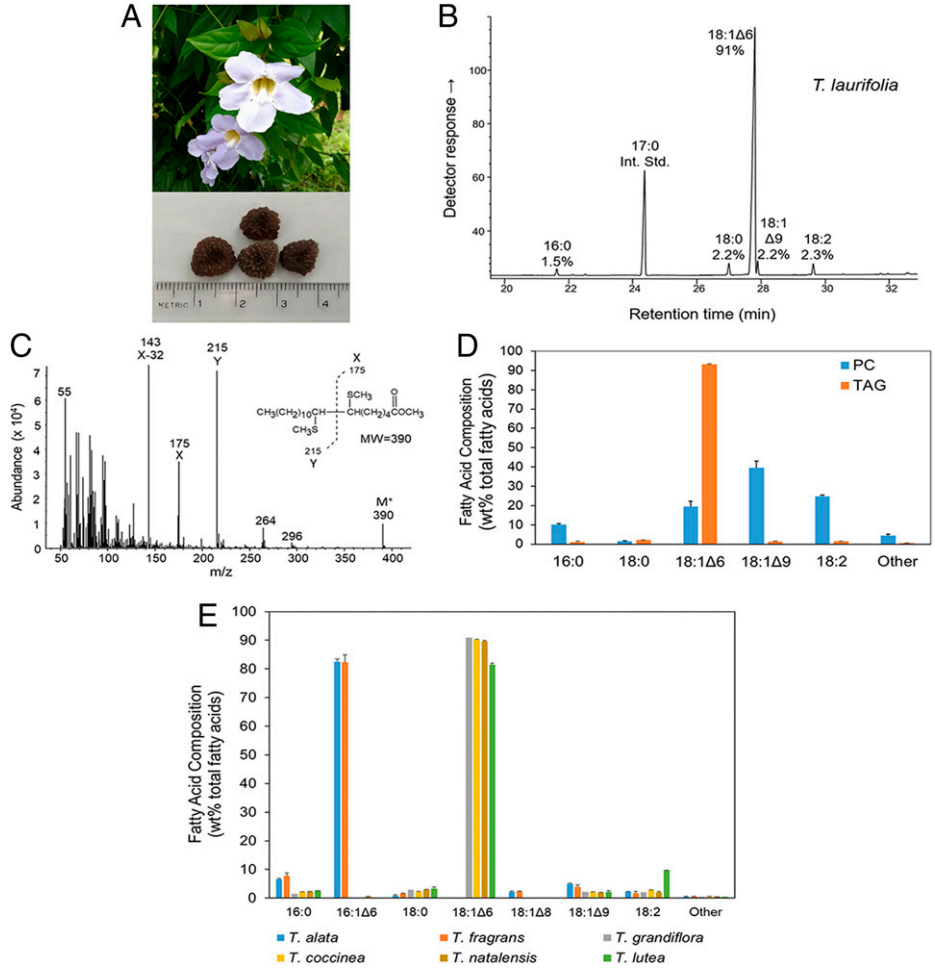

Fig. 1. Identification of petroselinic acid as the predominant seed FA of multiple *Thunbergia* species. (*A*) Flowers and seeds of *T. laurifolia*. (*B*) Gas chromatogram of isopropyl esters of FAs from the total lipid extract of *T. laurifolia* seeds with triheptadecanoin (17:0 TAG) added as an internal standard. (*C*) Mass spectral confirmation of petroselinic acid in *T. laurifolia* seeds analyzed as dimethyl disulfide derivatives of the methyl ester. (*D*) Comparison of the FA composition of TAG (orange) and PC (blue) fractions of *T. laurifolia* seed lipids. (*E*) FA composition of the total lipid of *T. alata* (blue), *T. fragrans* (orange), *T. grandiflora* (silver), *T. coccinea* (yellow), *T. natalensis* (brown), and *T. lutea* (green) seeds. Results of FA analyses in *D* and *E* are the average obtained from three to five independent biological replicates ± SD.

activities with 16:0-ACP and 18:0-ACP (*SI Appendix*, Fig. S5*C*). We focused primarily on comparing regiospecificities of mutants rather than detailed characterization of substrate affinities. In this regard, a prior study of the *T. alata* Δ6-16:0-ACP desaturase found that similar mutants were largely unaffected in substrate affinity, as indicated by relatively small changes in enzyme K_ms (19). Mutants appeared considerably less active than wild-type Δ6-18:0-ACP desaturase, likely a result of reduced k_{cat}, as has been shown or surmised for previous acyl-ACP desaturase mutants (19, 29). Mutations were informed through crystal structures of the castor Δ9-18:0-ACP desaturase (18) and English ivy Δ4-16:0-ACP desaturase (17).

One striking difference between the *T. laurifolia* and *T. alata* desaturases occurs at amino acids 183 and 184, which are at the bottom of the substrate binding pocket based on 3D structural information (19). The *T. laurifolia* enzyme and all known Δ9-18:0-ACP desaturases have Gly-Phe pair at these positions, while the *T. alata* enzyme has a bulkier Ala-Tyr pair (Fig. 2*B*). The *T. laurifolia* G183A F184Y desaturase mutant had increased 16:0-ACP desaturation activity, as predicted (Fig. 3 *A* and *B*). The products, however, had Δ9 unsaturation and no detectable Δ6 unsaturation. This mutant also displayed increased Δ9-18:0-ACP desaturation (Fig. 3 *A* and *B*). Indeed, all other mutants had increased Δ9 activity with both substrates (Fig. 3 *C*–*F*). Of note, the G183A/F184Y/S200N/L201T/G202A/Q275E mutant had only Δ9 desaturase activity and was most active with 18:0-ACP (Fig. 3*F*). Although conversion of *T. laurifolia* Δ6-18:0-ACP desaturase into a Δ9-18:0-ACP desaturase was successful, conversion of this enzyme into a Δ6-16:0-ACP desaturase was not. This suggests that other residues, including those that mediate surface interactions with the acyl-ACP substrate, contribute to regiospecificity.

We determined a crystal structure of the *T. laurifolia* Δ6-18:0-ACP desaturase at 2.0-Å resolution (Fig. 3*G* and *SI Appendix*, Figs. S6 and S7 and Table S1). As shown in Fig. 3*H*, amino acids mutated as described above were mapped on this structure. The lack of a cocrystal structure with an acyl-ACP substrate precluded definitive identification of residues that control regiospecificity. One notable observation was a Lys residue at amino acid 257 in the *T. laurifolia* desaturase that is exposed on the surface adjacent to the substrate binding cavity (Fig. 3*I* and *SI Appendix*, Fig. S7). This analogous residue in the *T. alata* Δ6-16:0-ACP and milkweed (*Asclepias syriaca*) Δ9-16:0-ACP desaturases is a Met. However, similar to the *T. laurifolia* enzyme, this residue is primarily a Lys in known Δ9-18:0-ACP desaturases. Consistent with regiospecific influence by this amino acid, it was found that a K257M mutant of the *T. laurifolia* Δ6-18:0-ACP desaturase produced Δ6 and Δ9 products, as well as an 18:0-ACP product with

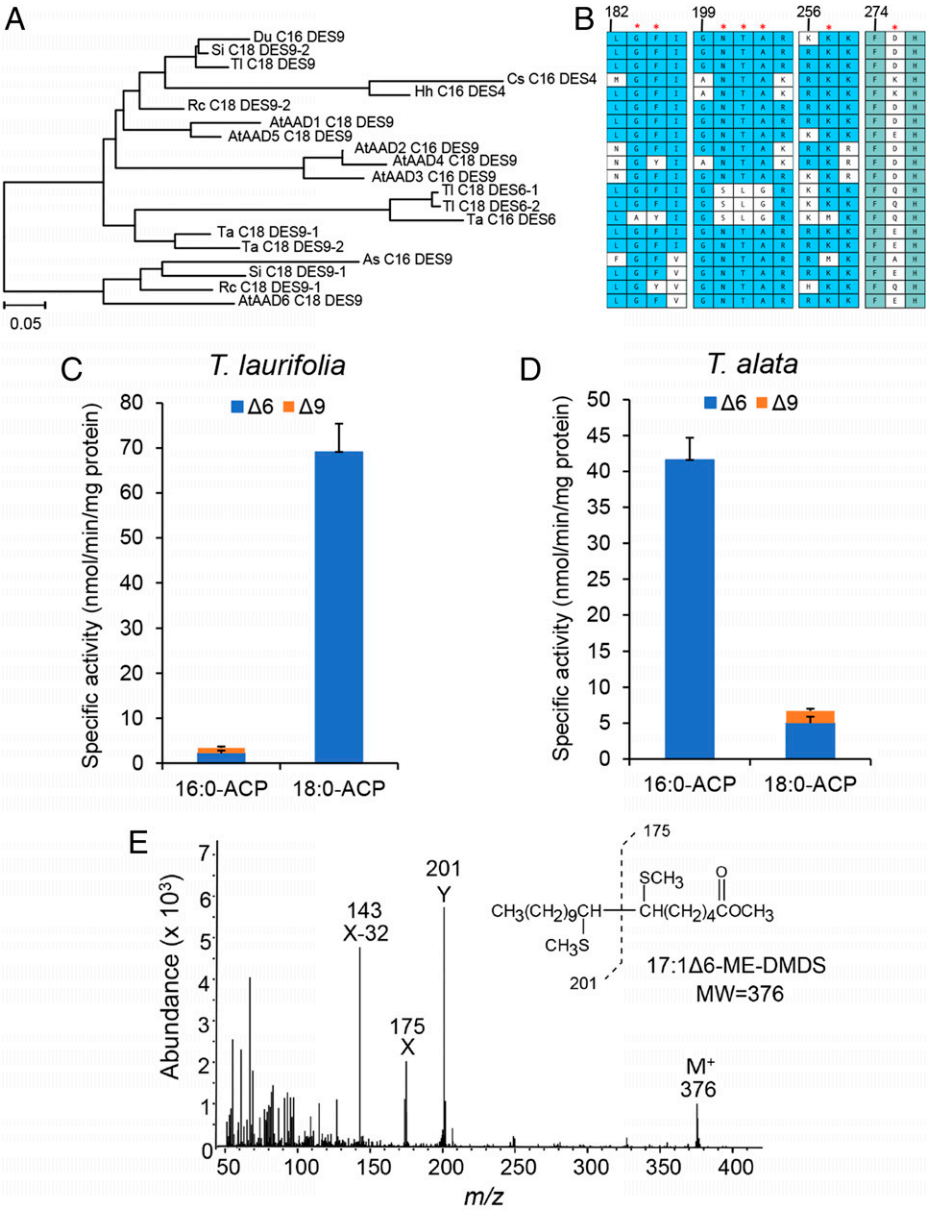

Fig. 2. Phylogeny and in vitro activities of Δ6 desaturases of *T. alata* and *T. laurifolia*. (*A*) Unrooted phylogenetic tree showing the close relationship of the two *T. laurifolia* desaturases with the *T. alata* Δ6-16:0-ACP desaturase. (*B*) Multiple alignment with asterisks showing the conservative residues between different desaturases in *A*. Green shading indicates 100% amino acid sequence identify; blue shading shows the consensus match; and white identicates mismatch from the consensus. These residues were targeted for mutagenesis to understand their contributions to the variant activity of the *Thunbergia* desaturases (see Fig. 4). (*C* and *D*) Comparison of activities and regiospecificities of Δ6 desaturases from *T. laurifolia* and *T. alata* with 16:0- and 18:0-acyl-ACP substrates. Values are averages obtained from three independent enzyme assays ± SD. (*E*) Mass spectrum of dimethyl disulfide derivatives of FA methyl ester of products from assay of *T. laurifolia* desaturase with 17:0-ACP to confirm production of Δ6 unsaturated product. Species, desaturases, and gene identifiers or GenBank accession numbers for acyl-ACP desaturases shown in *A*: AtAAD1: *A. thaliana* AAD1 AT5G16240; AtAAD2: *A. thaliana* AAD2 AT3G02610; AtAAD3: *A. thaliana* AAD3 AT5G16230; AtAAD4: *A. thaliana* AAD4 AT3G02620; AtAAD5: *A. thaliana* AAD5 AT3G02630; AtAAD6: *A. thaliana* AAD6 AT1G43800; Cs C16 DES4: *C. sativum* Δ4-16:0-ACP desaturase, P32063.1; Hh C16 DES4: *H. helix* Δ4-16:0-ACP desaturase, AAY46941.1; Rc C18 DES9-1: *R. communis* Δ9-18:0-ACP desaturase, NP_001310674.1; Rc C18 DES9-2: *R. communis* Δ9-18:0-ACP desaturase, NP_001310638.1; Du C16 DES9: *Dolichandra unguis-cati* Δ9-16:0-ACP desaturase, AAC05293.1; Si C18 DES9-1: *Sesamum indicum* Δ9-18:0-ACP desaturase, XP_011074783.1; Si C18 DES9-2: *S. indicum* Δ9-18:0-ACP desaturase, XP_011091536.1; Ta C18 DES9-1: *T. alata* Δ9-18:0-ACP desaturase, AAA61559.1; Ta C18 DES9-2: *T. alata* Δ9-18:0-ACP desaturase, AAA61560.1; As C16 DES9: *A. syriaca* Δ9-16:0-ACP desaturase, AAC49719.1; Ta C16 DES6: *T. alata* Δ6-16:0-ACP desaturase, Q41510.1; Tl C18 DES6-1: *T. laurifolia* Δ6-18:0-ACP desaturase, OL757550; Tl C18 DES6-2: *T. laurifolia* Δ6-18:0-ACP desaturase, OL757551; Tl C18 DES9: *T. laurifolia* Δ9-18:0-ACP desaturase, ON393910.

mobility above the Δ9 product on argentation TLC (Fig. 3*J*). This was the only product detected with 16:0-ACP. Expression of this mutant in an *E. coli* unsaturated FA auxotroph resulted in 16:1Δ10 production as determined by GC-MS (*SI Appendix*, Fig. S8), consistent with TLC mobility of desaturation products. In a second mutant that combined K257M substitution with G183A/F184Y substitutions, while production of the Δ10 isomer was maintained with 16:0- and 18:0-ACP, no Δ6 product was detected with 18:0-ACP (Fig. 3*K*). Notably, Δ10 activity has not been previously described for acyl-ACP desaturases. These findings support the utility of the 3D structure of the *T. laurifolia* Δ6-18:0-ACP desaturase for understanding acyl-ACP desaturase function and for generating novel unsaturation products.

Metabolic Engineering with Δ6 Desaturases and Other *Thunbergia* Genes. We examined the utility of *Thunbergia* species as a source of genes for metabolic engineering of FA composition of plant oils and bacteria (*SI Appendix*, Fig. S9). For plant-based

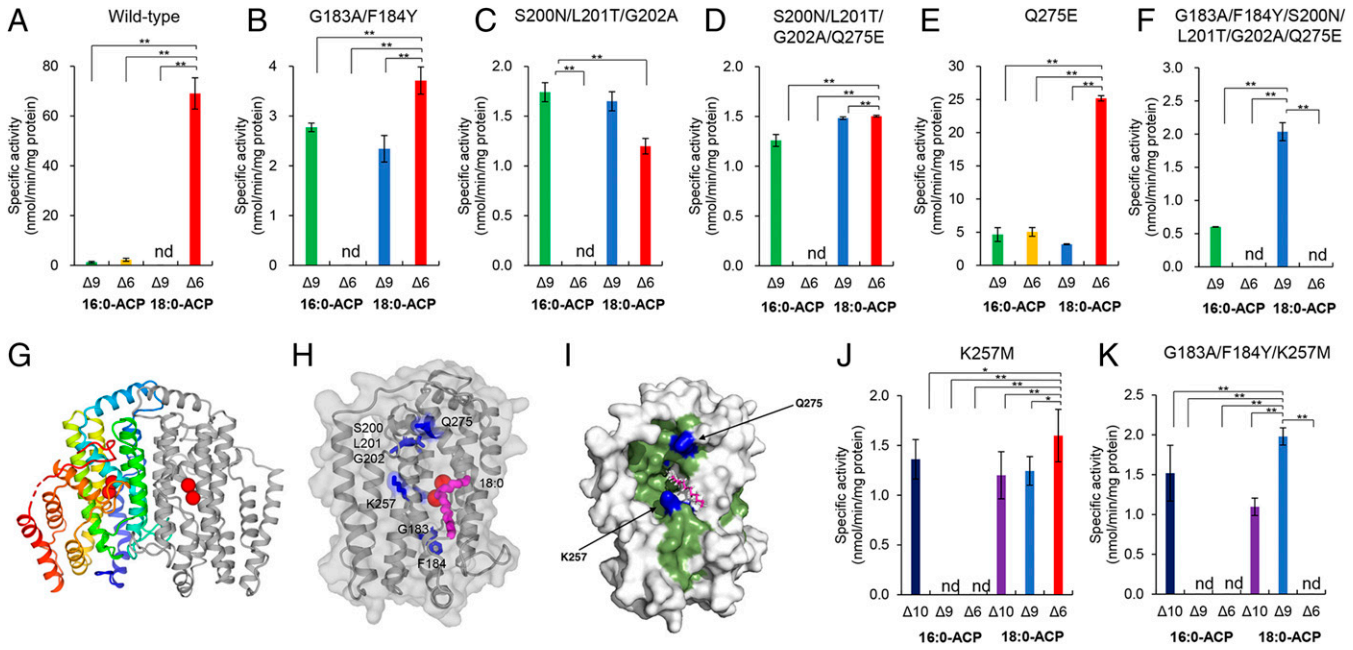

Fig. 3. Structure-guided mutagenesis of *T. laurifolia* Δ6-18:0-ACP desaturase for altered regiospecificity. (*A–F*) In vitro activity of *T. laurifolia* Δ6-18:0-ACP desaturase mutants that are designed based on amino acid sequence differences with *T. alata* Δ6-16:0-ACP desaturase and canonical Δ9-18:0-ACP desaturases. The relative production of Δ6 and Δ9 desaturation products is shown. (*G*) Structure of the *T. laurifolia* Δ6-18:0-ACP desaturase dimer determined at 2.0-Å resolution. (*H*) *T. laurifolia* Δ6-18:0-ACP desaturase crystal structure with the key amino acids labeled, (*I*) *T. laurifolia* Δ6-18:0-ACP desaturase structure in the surface model shows the K257 and Q275 at the bottom and top for the substrate pocket opening. (*J*) In vitro activity of K257M and (*K*) G183A/F184Y/K257M Δ6-18:0-ACP desaturase mutants. Data in *A–F*, *J*, and *K* are the averages ± SD from three independent assays (*$P < 0.05$, **$P < 0.01$, Student's *t* test). nd, not detected. Confirmation of Δ10 desaturation product is shown in *SI Appendix*, Fig. S8.

studies, we expressed cDNAs for the *T. laurifolia* and *T. alata* desaturases in the oilseed camelina (*Camelina sativa*) to compare in planta activities of these desaturases. cDNAs were expressed under the control of seed-specific promoter and linked to a constitutively expressed DsRed marker for visual selection of transgenic seeds. Multiple T_1 lines were obtained for each desaturase that produced Δ6 unsaturated FAs and their elongation products, which were advanced to the T_2 and T_3 generations. Homozygous T_3 seeds of the top-producing *T. laurifolia* Δ6-18:0-ACP desaturase line indicated ∼3% FA content accumulated as petroselinic acid, along with the elongation products 20:1Δ8 and 22:1Δ10 that comprised ≤6% of total FAs (Fig. 4*A* and *SI Appendix*, Figs. S10 and S11). Homozygous T_3 seeds from lines producing the highest levels of unusual monounsaturated FAs from the *T. alata* Δ6 desaturase accumulated only trace amounts of 16:1Δ6, instead accumulating elongation products of this FA: 18:1Δ8, 20:1Δ10, and 22:1Δ12, with double-bond positions confirmed by GC-MS (Fig. 4*B* and *SI Appendix*, Fig. S10). This appears analogous to the biosynthesis of petroselinic acid in Apiaceae seeds, where almost all of the initial 16:1Δ4 desaturation product is elongated to petroselinic acid (22). The *T. alata* Δ6-16:0-ACP desaturase product and its elongated forms accounted for ≥19% of total FAs of engineered seeds. To determine if 16:1Δ6 is elongated via plastid 3-ketoacyl-ACP synthase activity (KAS I or II) or from endoplasmic reticulum (ER) FA elongation via *FATTY ACID ELONGASE1* (*FAE1*)-encoded 3-ketoacyl-CoA synthase (KCS), *T. alata* desaturase was expressed in a camelina background with interfering RNA (RNAi) suppression of *FAE1* (30). Similar to the wild-type camelina seed phenotype, T_2 DsRed$^+$ seeds from three independent lines accumulated primarily 18:1Δ8, accounting for 16% of total FAs, and only trace amounts of 16:1Δ6 (Fig. 4*B*). However, large reduction in the C20 elongation product and no detectable 22:1Δ12 was observed. This is consistent with plastid elongation of 16:1Δ6-18:1Δ8 as ACP esters via KAS I or II and subsequent ER elongation of 18:1Δ8 as CoA esters by the ER pathway via the *FAE1*-encoded KCS.

Past studies of the Apiaceae Δ4 desaturation pathway suggested that narrow substrate specificity of typical acyl-ACP thioesterases limits petroselinic acid release from ACP and restricts petroselinic production in transgenic oilseeds (31). Given the increased petroselinic acid content of *T. laurifolia* seeds, developing *T. laurifolia* seeds were surveyed using PacBio-generated transcriptomic data to identify acyl-ACP thioesterases with high specificity for petroselinoyl-ACP. We identified cDNAs for two FatB and one FatA homologs, and coexpressed each under the seed-specific promoters along with *T. laurifolia* Δ6-18:0-ACP desaturase on a single binary vector with DsRed screening. No increase in petroselinic acid content of DsRed seeds was observed in lines coexpressing *FatB* cDNAs relative to lines expressing the desaturase alone (*SI Appendix*, Fig. S12). In contrast, DsRed$^+$ seeds from 30 independent events engineered for coexpression of the *T. laurifolia* FatA and Δ6-18:0-ACP desaturase accumulated petroselinic acid and its elongation products 20:1Δ8 and 22:1Δ10 to ∼18% of total FAs, an approximately three-fold increase compared to seeds expressing only the *T. laurifolia* desaturase (Fig. 4*A* and *SI Appendix*, Fig. S13). Of these FAs, petroselinic acid accounted for ∼12% of the total in the top T_2 coexpression lines, compared to ∼2% petroselinic acid in seeds expressing *T. laurifolia* desaturase alone. In contrast, coexpression of the *T. alata FatA* homolog in the top-producing *T. alata* Δ6 desaturase line resulted in little to no enhancement in production of 16:1Δ6 and its elongation products (*SI Appendix*, Fig. S12). Camelina seeds with ≤20% petroselinic acid were subsequently identified in the T_2 generation from combining seed-specific expression of transgenes for *T. laurifolia* Δ6-18:0-ACP desaturase, FatA, lysophosphatidic acid acyltransferase

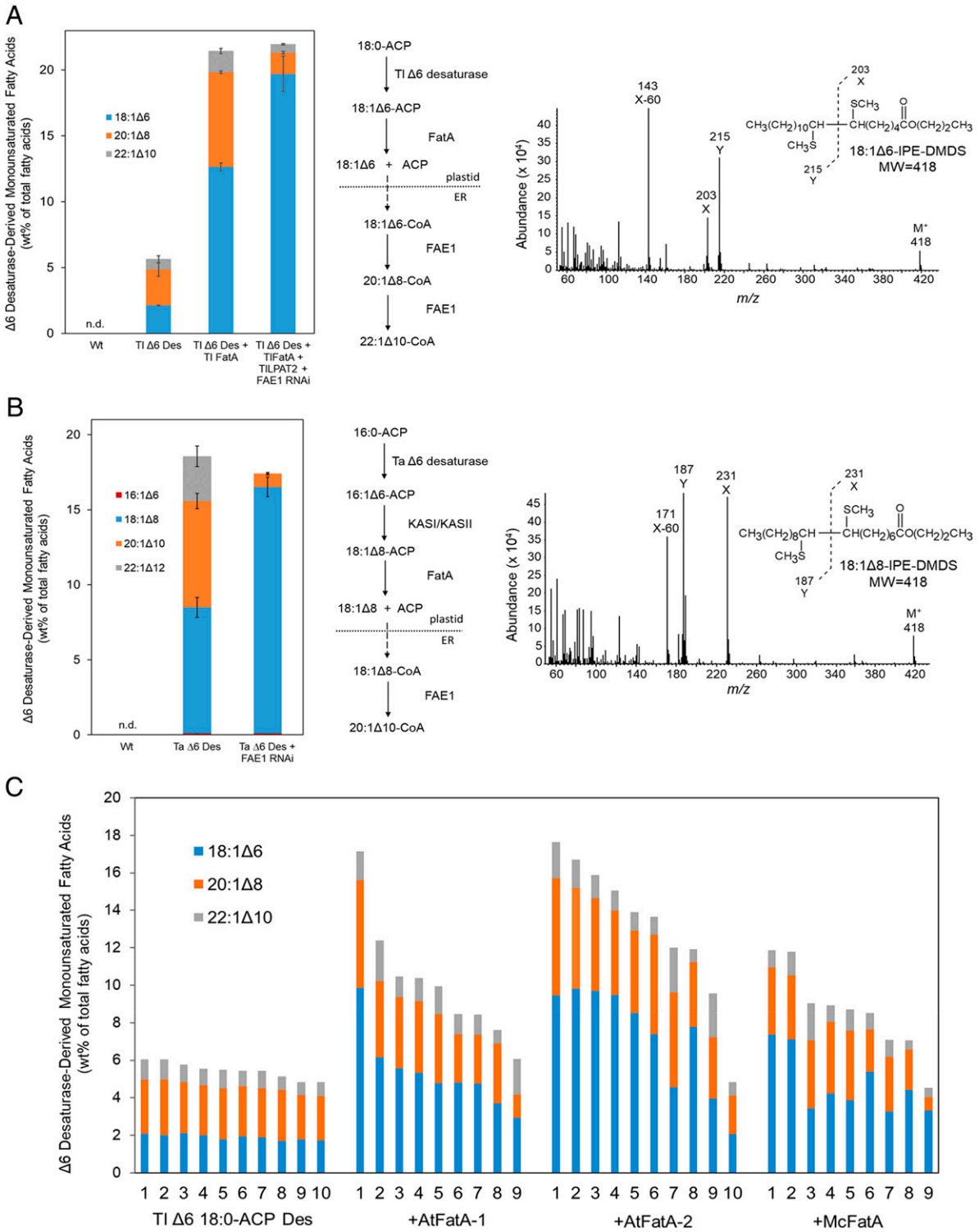

Fig. 4. Metabolic engineering for production of oils containing petroselinic acid and other Δ6 FA desaturase-derived FAs in camelina seeds by expression of genes from *T. laurifolia* or *T. alata*. (*A*) Relative amounts of Δ6 desaturase-derived monounsaturated FAs in the total FAs from homozygous T_3 camelina seeds of top-producing line engineered for expression of the *T. laurifolia* Δ6-18:0-ACP desaturase alone (Tl Δ6 Des) or coexpression with a *T. laurifolia* FatA cDNA (Tl Δ6 Des + TlFatA). Also shown are relative amounts of Δ6 desaturase-derived monounsaturated FAs in the total FAs of T_2 camelina DsRed$^+$ seeds from top producing line engineered for coexpression with a *T. laurifolia* Δ6 desaturase, FatA and LPAT2 cDNAs with *FATTY ACID ELONGASE1 FAE1* RNAi (Tl Δ6 Des + TlFatA + TlLPAT2 + FAE1 RNAi). n.d., not detected. (*B*) Relative amounts of Δ6 desaturase-derived monounsaturated FAs in the total FAs from homozygous T_3 camelina seeds of top-producing line engineered for expression of the *T. alata* Δ6-16:0-ACP desaturase alone (Ta Δ6 Des) or in a *FA ELONGASE1 FAE1* RNAi background (Ta Δ6 Des + FAE1 RNAi). Data in *A* and *B* are the averages of measurements of seeds from three to five independent plants for each line ± SD. Proposed biosynthetic pathways for the production of Δ6 desaturase-derived monounsaturated FAs and mass spectral confirmation of the major products from transgenic expression of *T. laurifolia* and *T. alata* genes are also shown. Double-bond positions were determined by GC-MS analysis of dimethyl disulfide derivatives of FA isopropyl esters. n.d., not detected. (*C*) Comparison of Δ6 desaturase-derived monounsaturated FA production in T_2 DsRed$^+$ camelina seeds expressing the *T. laurifolia* Δ6-18:0-ACP desaturase alone (Tl Δ6-18:0-ACP Des) or coexpressed with the *Arabidopsis* FatA-1 (+AtFatA-1), *Arabidopsis* FatA-2 (+AtFatA-2), or *M. charantia* FatA (+McFatA).

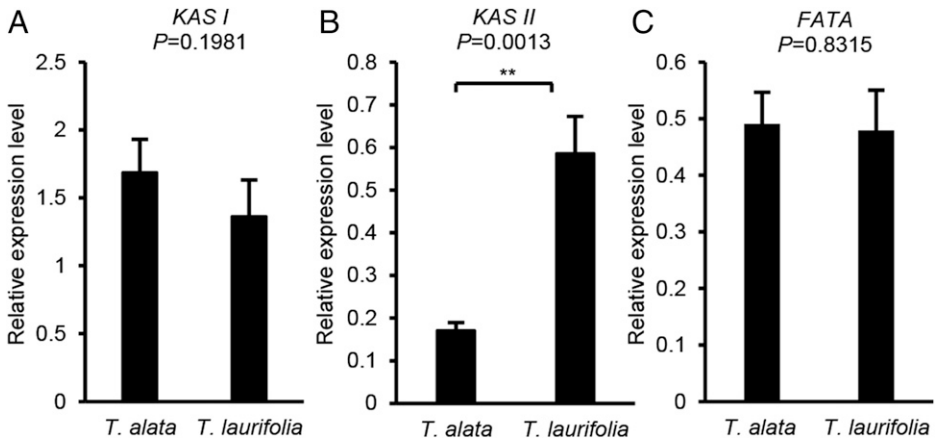

Fig. 5. Expression analysis of genes for KAS I, KAS II, and FatA in developing *T. alata* and *T. laurifolia* seeds. (*A*–*C*) Results averages from three independent qPCR experiments ± SD (**$P < 0.01$, Student's *t* test).

2 (LPAT2), and seed-specific suppression of a camelina *FAE1*-targeted RNAi cassette (Fig. 4*A* and *SI Appendix*, Figs. S11 and S14). This is approximately five-fold more than previously reported for petroselinic acid production in transgenic seeds using enzymes from the Apiaceae Δ4-16:0-ACP desaturation pathway (24).

Thioesterases for Enhanced Petroselinic Acid Production. In vitro thioesterase assay of recombinant *T. laurifolia FatA* expressed in *E. coli* was used to determine substrate preference for 18:1Δ6-ACP versus 18:1Δ9-ACP. This enzyme was found to be 10-fold more active with 18:1Δ9-ACP compared to 18:1Δ6-ACP and similar to that of recombinant *Arabidopsis* FatA-1 (*SI Appendix*, Fig. S15). This finding suggested that the *T. laurifolia* FatA is not specialized for petroselinic acid release from ACP and that the increase in petroselinic acid production from its overexpression in camelina seeds is the result of increased in vivo FatA activity from seed-specific expression of the transgene. We hypothesized that a similar increase in petroselinic acid production in camelina could be achieved by expression of a FatA transgene from any plant source. We therefore coexpressed the *T. laurifolia* Δ6-18:0-ACP desaturase and FatAs from *Arabidopsis* and *Momordica charantia* under the control of seed-specific promoters. With each of these FatAs, production of petroselinic acid and its elongation products were increased by two to three-fold relative to expression of the Δ6-18:0-ACP desaturase alone. The increase in *Arabidopsis* FatA-2 expression was consistently the highest of the three FatAs tested over seeds from independent events and similar to that obtained using the *T. laurifolia* FatA (Fig. 4*C*). This finding suggests that petroselinic acid production in transgenic seeds is limited by the total *in vivo* FatA activity rather than the substrate specificity of this enzyme.

Divergent Evolution of Extreme Δ6 Monoene Production in *T. alata* and *T. laurifolia* Seeds. To better understand the near lack of elongation of 16:1Δ6-ACP in *T. alata* seeds and the near complete elongation of this intermediate in engineered camelina seeds, we compared expression levels of *KASI*, *KASII*, and *FatA* genes in developing *T. alata* and *T. laurifolia* seeds. For these measurements, we used identical primers for *T. alata* and *T. laurifolia* genes that were designed from conserved sequences in genes from both species. Similar expression levels of *KASI* and *FatA* were detected in seeds of the two species (Fig. 5 *A* and *C*). However, *KASII* expression was approximately three-fold lower in *T. alata* compared to *T. laurifolia* seeds (Fig. 5*B*), consistent with the hypothesis that *T. alata* seeds have reduced capacity for 16:1Δ6-ACP elongation. We also measured expression of these genes in developing camelina seeds. The use of different primer sets precluded direct quantitative comparison with the corresponding *T. alata* and *T. laurifolia* genes. Nevertheless, the ratio of *KASII:KASI* expression in camelina seeds (0.5) was higher than that in *T. alata* (0.1) and *T. laurifolia* (0.4) seeds (*SI Appendix*, Fig. S16), consistent the capacity of camelina seeds for nearly complete elongation of 16:1Δ6-ACP to form 18:1Δ8-ACP (Fig. 4*B*).

Discussion

The findings presented here arose from our initial discovery that the unusual monounsaturated FA petroselinic acid accounts for ∼92% of seed oil FAs of at least four *Thunbergia* species. The natural occurrence of a single FA at such high levels in a seed oil is rare in the plant kingdom. Other examples include castor oil with ≥89% ricinoleic acid (32), *Cuphea pulcherrima* oil with ∼94% octanoic acid (7), and the oil produced in *Carthamus tinctorius L.* (safflower) mutants with ∼90% oleic acid (33). Our findings contrasted with a previous report of the occurrence of 16:1Δ6 to amounts of 82% in *T. alata* seed oil (26). The differences in unusual FA composition between *Thunbergia* species allowed for exploration of the biochemical basis for an atypical example of variant FA biosynthesis and metabolism and its divergence within this genus. It also enabled us to tap these species as gene sources for metabolic engineering of enhanced-value FA production in plants and microbes.

We show that the divergence in monounsaturated FA composition between *T. laurifolia* and *T. alata* seeds arises primarily from differences in substrate specificity of their Δ6 desaturases. Our phylogenetic analyses are most consistent with the recent evolution of the *Thunbergia* Δ6-18:0-ACP desaturase from the canonical to Δ9-18:0-ACP desaturase and subsequent evolution of the Δ6-16:0-ACP desaturase found in *T. alata* and likely *T. fragrans* (*SI Appendix*, Fig. S4). Our mutagenesis studies identified amino acid residues that can convert *T. laurifolia* Δ6-18:0-ACP desaturase to Δ9-18:0-ACP desaturase, but were unable to convert Δ6-18:0-ACP desaturase by mutagenesis to *T. alata*-type Δ6-16:0-ACP desaturase. A previous study indicated that mutations of residues A183 and Y184 in the *T. alata* Δ6-16:0-ACP desaturase to G183 and F184 found in the *T. laurifolia* Δ6-18:0- ACP desaturase and all known Δ9-18:0-ACP desaturases generated a Δ6 desaturase that is equally active with 16:0- and 18:0-ACP (19). These residues are at the

bottom of the substrate binding pocket based on our crystal structures for the *T. laurifolia* enzyme and the castor Δ9-18:0-ACP desaturase (19). This mutation is predicted to expand the volume of the binding pocket to accommodate the longer 18:0-ACP substrate. The converse mutation in the *T. laurifolia* Δ6-18:0-ACP desaturase increased the relative activity of the enzyme with 16:0-ACP, but the product had almost exclusively Δ9 unsaturation. This finding suggests that possible evolution of the *T. laurifolia* Δ6-18:0-ACP desaturase to the Δ6-16:0-ACP desaturase involves amino acid changes at the bottom and surface of the binding pocket and likely elsewhere affecting the positioning of 16:0-ACP in the required configuration for Δ6 desaturation. Consistent with the importance of surface residues for substrate positioning, the K257M mutation in the Δ6-18:0-ACP desaturase, which is predicted to affect surface interactions with the acyl-ACP substrate based on crystal structure, yielded an enzyme with not only Δ9 but also Δ10 regiospecificity. The latter activity is not known to naturally exist. The availability of the *T. laurifolia* Δ6-18:0-ACP desaturase three dimensional-structure generated in this study should provide greater clarity on the determination of the regiospecificity of acyl-ACP desaturases, particularly by cocrystallization with acyl-ACP substrates as well as computational structural modeling, as recently shown by use of the *T. alata* Δ6-16:0-ACP desaturase structure (34).

Petroselinic acid has been a biotechnological production target because it can serve as a precursor via oxidative cleavage for lauric acid, a surfactant, and adipic acid, a nylon 6,6 feedstock (35, 36). Furthermore, oils enriched in petroselinic acid have been touted as low caloric oils because they are poorly digested by pancreatic lipases compared to typical vegetable oils (35, 37). These oils, in contrast to oleic acid-rich oils, are solid at room temperature and have potential for margarine production without *trans*-fat–generating hydrogenation (35). Oilseed-based metabolic engineering for petroselinic acid production has previously been attempted through a pathway in Apiaceae and Araliaceae that uses a Δ4-16:0-ACP desaturase and subsequent ACP-linked elongation (21). Transgenic expression of the coriander Δ4-16:0-ACP desaturase in *Arabidopsis* seeds resulted in oils with ≤2.5% petroselinic acid and its 16:1Δ4 precursor (24). The Δ6-18:0-ACP desaturase-mediated pathway in *T. laurifolia* seeds offers an alternative route for engineering petroselinic acid production. Expression of the *T. laurifolia* Δ6-18:0-ACP desaturase in camelina seeds yielded ≤6.5% of petroselinic acid and its C20 and C22 elongation products, of which ∼40% was present as petroselinic acid (≤2.5% of total fatty acids).

A suspected limitation of the Δ4-16:0-ACP desaturase pathway is a thioesterase that is specialized for cleavage of petroselinoyl-ACP (31). While we failed to identify a thioesterase with elevated in vitro activity with petroselinoyl-ACP from a *T. laurifolia* seed transcriptome, we discovered instead that enhanced expression of a FatA thioesterase from *T. laurifolia* and unrelated species was sufficient to enhance production of petroselinic acid and its elongation products by approximately three-fold in engineered camelina seeds. These findings confirm that a major bottleneck in petroselinic acid production in transgenic oilseeds is its cleavage from ACP, but this can be overcome with increased expression of a nonspecific FatA. Building on this finding, we engineered petroselinic acid production to ∼20% of total camelina FA seed by suppressing *FAE1* RNAi to minimize petroselinic acid elongation and expression of a *T. laurifolia LPAT2* to enhance petroselinic acid incorporation into the *sn*-2 position of TAG. The latter experiment was a proof-of-concept experiment that achieved the highest level of petroselinic acid content reported to date in engineered oilseed and demonstrates the feasibility of petroselinic acid metabolic engineering in oleaginous plant and microbial cells.

Our efforts to reconstruct biosynthetic pathways for petroselinic and sapienic acids in camelina also provided clues about the evolution of extreme production of these FAs in *Thunbergia*. Experimental results suggest that the ability of *T. laurifolia* seeds to produce high levels of petroselinic acid is an evolutionary consequence of: 1) a Δ6-18:0-ACP desaturase, 2) elevation of FatA activity, and 3) specialized downstream enzymes (e.g., LPAT2) for TAG production using petroselinoyl-CoA substrates. However, in camelina metabolic engineering studies, FatA overexpression did not increase 16:1Δ6 production from expression of the *T. alata* Δ6-16:0-ACP desaturase. Instead, 16:1Δ6-ACP appears to be preferentially and predominantly elongated to 18:1Δ8-ACP by KAS activity in engineered camelina seeds. This suggests that 16:1Δ6-ACP is a poor substrate for FatA thioesterase activity, despite increased *FatA* expression. Given the high 16:1Δ6 and low 18:1Δ8 content in *T. alata* seeds (26), these observations suggest that *KASII* is suppressed in *T. alata* seeds relative to camelina seeds. Consistent with this, we determined that *KASII* is expressed at approximately three-fold lower levels in *T. alata* compared to *T. laurifolia* seeds. From these observations, we can hypothesize that the evolutionary divergence in *Thunbergia* that gave rise to sapienic acid production and evolution of the Δ6-16:0-ACP desaturase was driven by reduced flux through KASII and cell requirements for unsaturated FAs. Overall, our results highlight the value of the *Thunbergia* genus for gaining insights into extreme FA metabolic evolution and its influence on divergent biochemical outcomes.

Materials and Methods

FA Compositional Analyses of *Thunbergia* sp. and Engineered Camelina Seeds. Seeds of *T. laurifolia*, *T. grandiflora*, *T. alata*, *T. fragrans*, *T. natalensis*, *T. lutea*, and *T. coccinea* obtained from eBay vendors were ground using a mortar and pestle, and 20 to 100 mg of seed powder were weighed into glass screw-cap test tubes for total lipid extraction using the Bligh and Dyer (38) method. The internal standard triheptadecanoin (17:0-TAG) dissolved in toluene (20 mg/mL) and 3 mL of chloroform:methanol (1:2 [vol/vol]) was added to each tube. The ground seeds were homogenized using an Omni THq stainless steel rotary grinder and incubated in the extraction solvent at 25 °C for 1 h. One milliliter of chloroform and 1.8 mL of water were added to each tube. Following shaking and centrifugation at 1,000 × *g* in a clinical centrifuge for 10 min, the lower layer containing the total lipid extract was transferred to another glass screw-cap tube. Approximately 10% of the total lipid extract was dried under N_2 in a glass screw-cap test tube (13 × 100 mm). The extract was transesterified by heating at 98 °C for 1 h in 1.25% sulfuric acid in isopropanol (39). Following cooling, FA isopropyl esters (FAIPEs) were extracted by addition of 1.5 mL water and 2 mL heptane, mixing, and centrifugation. FAIPEs in the heptane layer were analyzed by gas chromatography using a HP-88 column (60-m length × 0.25-mm inner diameter, 0.2-μm film thickness) with the oven temperature programmed from 100 °C to 230 °C at 2.5 °C/min. FAIPEs were also analyzed from the TAG fraction purified from the total lipid extract by silica solid phase extraction as described and from PC isolated from *T. laurifolia* seed lipids using solid-phase extraction and subsequent TLC, as described previously (40). Similar methods were used for FA analyses of engineered camelina seeds. For some studies, FA methyl esters were prepared from powdered seeds as previously described (41). TAG FA stereospecific analyses were conducted using lipase digestion, as described previously (41).

Determination of Double-Bond Positions of Monounsaturated FAs. Double-bond positions of monounsaturated FAs from *Thunbergia* sp. seeds were determined by GC-MS of dimethyl disulfide derivatives of the methyl or isopropyl esters of these FAs, as described previously (25).

Homology-Based Cloning of *T. laurifolia* acyl-ACP Desaturases. Total RNA was isolated from developing seeds of *T. laurifolia*, as described previously (42).

Total RNA (1 μg) was treated with DNase I (Invitrogen) and used to synthesize oligo(dT)-primed first-strand cDNA with the RevertAid first-strand cDNA synthesis kit (Thermo Scientific). Homology-based cloning was performed with a degenerate primer based on the *T. alata* Δ6-16:0-ACP desaturase coding sequence (*SI Appendix*, Table S2). The PCR product representing a portion of the full-length cDNA was cloned into the pCR-Blunt II-TOPO vector (Invitrogen) and sequenced. The full-length *T. laurifolia* Δ6-18:0-ACP desaturase coding sequence was obtained by 5′ and 3′ rapid amplification of cDNA ends (RACE) using the SMARTer RACE cDNA Amplification Kit (Clontech). Purified total RNA (1 μg) was used to synthesize cDNA for 5′ and 3′ RACE. Gene-specific primers were designed according to sequence results of the homology-based cloning described above (*SI Appendix*, Table S2). At least 10 clones were sequenced for each fragment.

Iso-Seq Library Preparation and PacBio Sequencing of *Thunbergia* Seed Transcriptomes. Total RNA samples from developing *T. laurifolia* and *T. alata* seeds from garden-grown plants were quantified using Qubit 2.0 Fluorometer (Life Technologies) and RNA integrities were checked with TapeStation 4200 (Agilent Technologies). Iso-Seq library preparations, sequencing reactions, and initial bioinformatics analysis were conducted at GENEWIZ, LLC. For Iso-Seq library construction, total RNA was converted into amplified full-length cDNA using the SMARTer PCR cDNA synthesis Kit (Clontech). The library for PacBio Sequel was constructed using SMRTbell Express Template Prep Kit 2.0 (PacBio). The library was bound to polymerase using the Sequel Binding Kit (PacBio) and loaded onto PacBio Sequel using the MagBead Kit V2 (PacBio). Sequencing was performed on 1 PacBio Sequel SMRT Cell 1M v3 (10-h movie time) per sample.

De Novo Reconstruction of *T. alata* and *T. laurifolia* Seed Transcriptomes. Iso-Seq v3 tools (v3.0.0, https://github.com/PacificBiosciences/IsoSeq) were used to reconstruct transcriptomes from PacBio sequences. The workflow included circular consensus sequence calling using "ccs", primer removal using "lima", trimming of poly(A) tails using "isoseq3 refiner", clustering and generation of consensus sequences using "isoseq3 cluster", and polishing using "isoseq3 polish".

Identification and Annotation of Protein Sequences from Seed Transcriptomes. Protein sequences coded by *T. alata* and *T. laurifolia* seed transcriptomes were predicted by taking the longest open reading frame from each transcript by ORF finder v0.4.3 (43). The protein sequences were annotated based on the reciprocal top hits using BLASTP (v2.8.1+) protein similarity search (44) against the *Arabidopsis thaliana* Araport11 transcriptome model (45). Additional search and analyses of the nucleotide and protein sequences of transcriptomes for each species were performed using the BLAST Web server locally set up using SequenceServer v1.10.0 (46).

Generation of Camelina Transgenic Lines. For expression of Δ6 desaturases in plants, the full-length coding sequence of the *T. alata* Δ6-16:0-ACP desaturase or the *T. laurifolia* Δ6-18:0-ACP desaturase was inserted into the binary vector pBinGlyRed3 under the control of the seed-specific glycinin-1 promoter (30). For coexpression of the Δ6 desaturases with cDNAs for *T. alata*, *T. laurifolia*, *Arabidopsis*, or *M. charantia* FatAs or FatBs, coding sequences were amplified from cDNA by PCR (*SI Appendix*, Table S2) and inserted into the vector pKMS2 using a *Not*I site under the control of the seed-specific soybean oleosin promoter (30). Each expression cassette was digested and inserted into the *Asc*I site of the pBinGlyRed3 vector (30) containing the *T. alata* or *T. laurifolia* Δ6 desaturase expression cassettes described above. In addition, the *TlLPAT2* cDNA was PCR amplified (*SI Appendix*, Table S2) and inserted into the NotI site of the BetaConHyg vector under control of a seed-specific promoter (α′ subunit of β-conglycinin) (30). The entire cassette was digested with AscI and ligated into the corresponding site of the previously described vector pBinGlyBAR1+cFAE1 RNAi (30) that contains a seed-specific camelina *FAE1* RNAi cassette to generate pBinGlyBAR1+cFAE1 RNAi+TlLPAT2. Constructs were introduced into *Agrobacterium tumefaciens* GV3101 by electroporation. Transformation of *C. sativa* (cv. Suneson) was performed by floral vacuum infiltration method and positive seeds were selected with DsRed protein fluorescence, as previously described (30, 47). Camelina lines were also generated by transformation of the pBinGlyBAR1+cFAE1 RNAi+TlLPAT2 vector into a homozygous line harboring a T-DNA for seed-specific *T. laurifolia* Δ6-18:0-ACP desaturase and *T. laurifolia* FatA cassettes. Transgenic lines were selected from these transformations by resistance to glufosinate (30). Ten to 20 independent transgenic lines were selected for each construct and maintained under greenhouse conditions as described previously (20, 30). Independent transgenic lines were advanced to subsequent generations based on seed content of Δ6 unsaturated FAs and elongation products.

Preparation of *E. coli* Expression Constructs for Δ6-18:0-ACP Desaturase Mutants. All site-specific mutations in the coding sequence of the Δ6-18:0-ACP desaturase lacking the plastid transit peptide were introduced by extension and amplification of overlapping PCR using Phusion polymerase (ThermoFisher) (*SI Appendix*, Table S2). The mature peptide of the wild-type and mutant acyl-ACP desaturases generated from overlapping PCRs were cloned into the *Nde*I site of the expression vector pET3a under the T7 RNA polymerase promoter. PCR primers used to generate mutants are listed in *SI Appendix*, Table S2.

Cloning, Protein Purification, and Crystallization of Δ6-18:0-ACP Desaturase. The *T. laurifolia* Δ6-18:0-ACP desaturase sequences lacking its transit peptide and an additional truncation of 11 amino acids after the transit peptide cleavage site was cloned by PCR from CDS1 and fused with an N-terminal 6xHis tag and tobacco etch virus (TEV) protease recognition site by infusion (N-11 truncation-6xHis-TEV). N-11 truncation N-6xHis-TEV was cloned into pET28a for expression in *E. coli* and purified using nickel-nitrilotriacetic acid (Ni-NTA) affinity chromatography (Qiagen). The His-tag was removed by TEV protease digestion, and the reaction mix was passed through the Ni-NTA column a second time to remove noncleaved protein. The N-11 truncation desaturase in the flow through was collected, concentrated, and further purified using an HPLC system with a TSK gel G3000SW column (Tosoh Bioscience) size-exclusion chromatography. Fractions enriched to near homogeneity (>95%) were pooled and concentrated with minimal loss. Enzymatic activity of the *T. laurifolia* N-11 truncation desaturase was confirmed by in vitro assay in which the 18:0-ACP substrate was converted to Δ6-18:1-ACP, as identified by GC-MS analysis of its dimethyl disulfide derivative. The N-11 truncation-6xHis-TEV desaturase construct, which yielded protein with increased solubility relative to the mature desaturase polypeptide, was identified after protein expression, and purification trials for 18 separate constructs. After crystallization screening and optimization of conditions, 0.1M BICINE, 2 to 4% (vol/vol) 1,4-Dioxane, 10% (wt/vol) polyethylene glycol 20,000 produced diffraction quality crystals.

X-Ray Crystallography. Diffraction data were collected at the NSLS-II beamline FMX (17ID-2) at 100 K using an Eiger 16 M detector (48). We collected data at an X-ray wavelength of 1.743 Å. A total of 1,080 frames were collected from a single crystal with a rotation angle of 0.2° per frame. Diffraction data were indexed and integrated using DIALS (49), then scaled and merged using CCP4 programs POINTLESS and AIMLESS (50, 51). The data collection and data processing statistics are listed in *SI Appendix*, Table S1. The structure was solved by molecular replacement using Phaser (52) with PDB code ID 1AFR (18) as a starting model. Model building and refinement were performed in COOT (53) and PHENIX.REFINE (54, 55), respectively. The stereochemistry of the refined structures was validated with PROCHECK (56) and MolProbity (57) for quality assurance. The refinement statistics for the two datasets are shown in *SI Appendix*, Table S1.

***E. coli* Expression and Purification of Δ6-18:0-ACP Desaturase and Mutants.** pET3a vectors harboring wild-type and mutated Δ6-18:0-ACP desaturases were introduced and expressed in *E. coli* BL21 (DE3) cells, and assay of the high-purity protein was performed as described previously with some modifications (19). Three-liter cultures of *E. coli* cells were induced by addition of isopropylthio-β-galactoside (IPTG; 0.4 mM) while the OD_{600} was between 0.4 and 0.5, and then grown at 16 °C overnight. Bacterial cells were harvested by centrifugation and resuspended in 50 mL of a buffer consisting of 6.7 mM MES/6.7 mM Hepes/6.7 mM MOPS (pH 7.0) and 1 mM phenylmethylsulfonyl fluoride and then were lysed by lysozyme treatment and ultrasonication. The resulting soluble protein was first eluted from the S resin with gradient of 20-column volumes from 0 to 600 mM NaCl in 6.7 mM MES/6.7 mM Hepes/6.7 mM MOPS (pH 7.0), and then high-purity protein was obtained by gel filtration using the Superdex 200 column (GE Healthcare Life Sciences) interfaced with an FPLC system (Bio-Rad). Functional expression of wild-type and mutants in the pLac3 vector in the previously described *E. coli* unsaturated FA auxotrophic cell line MH13/pAnFd (58). FAs were analyzed from IPTG-induced cells by GC-FID as isopropyl esters and double bond positions of monounsaturated FAs determined by GC-MS as dimethyl disulfide derivatives (see above).

Acyl-ACP Desaturase Activity Assay. Acyl-ACP desaturation assays were conducted as previously described in 100-μL reactions using 1-^{14}C- palmitoyl- or stearoyl-ACP (recombinant spinach ACP) substrates (19). Reactions were started with the addition of recombinant acyl-ACP desaturase and were conducted at room temperature (25 °C). The methyl ester derivative products and unreacted substrates were separated on a 10% $AgNO_3$ TLC (20 cm in height) and developed sequentially to heights of 10 and 20 cm in toluene in a TLC development chamber placed in a −20 °C radiation storage freezer. Radioactivity was detected by Typhoon FLA 7000 phosphorimaging system (GE Healthcare Life Sciences) and the percent conversion of the saturated substrate to unsaturated product was measured using ImageQuant software (19).

Acyl-ACP Thioesterase Expression in *E. coli* and Activity Assay. The coding sequences for the mature *T. alata* FatA (TaFatA), *T. laurifolia* FatA (TlFatA), and *Arabidopsis* FatA (AtFatA) were amplified using primers shown in *SI Appendix*, Table S2, ligated into the *Nde*I restriction site of pET3a, and transformed into *E. coli* BL21 (DE3) strain. Transformed colonies were cultured in liquid LB media containing 1% glucose and ampicillin selection. For protein induction, cultures were incubated with shaking at 200 rpm at 30 °C for 3 h in presence of 0.1 mM of IPTG with 3% glucose. Total crude protein was extracted in 1× Laemmli sample buffer (50 mM Tris·HCl pH 6.8, 2% SDS, 100 mM DTT, 10% glycerol). Each 20 μg of crude protein was loaded in 12% SDS/PAGE gel and stained by Coomassie blue dye. Total crude protein extracts were prepared by sonication (Qsonica Q55) in phosphate-buffered saline buffer containing 1 mM EDTA. After removal of cell debris, soluble proteins were assayed by incubation with 0.33 mM 1-^{14}C-acyl-ACP (petroselinoyl-ACP, 18:1Δ6 or oleoyl-ACP, 18:1Δ9; 55 Ci/mole) in 100 mM Tris (pH 8.5) buffer were incubated at 23 °C for 5 min, similar to the method described previously (31). Radiolabeled petroselinoyl-ACP was the gift of Joaquín J. Salas, Instituto de la Grasa, Seville, Spain, and John Ohlrogge, Michigan State University, East Lansing, MI, and prepared using chemically synthesized 1-^{14}C-petroselinic acid. The reaction was terminated by adding equal volume of 1 M acetic acid in isopropanol. Free FAs were extracted with heptane saturated with 50% (vol/vol) isopropanol, and supernatant from three extractions of each reaction was collected into scintillation vials. To measure residual acyl-ACP, a lower phase of reactant was added to a separate scintillation vial. Free FAs and immobilized acyl-ACP were dried under N_2 and dissolved in 10 mL of scintillation mixture (Bio-Safe II, Research Products International). Radioactivity was measured using liquid scintillation counting (Beckman Coulter LS6500).

Gene-Expression Analyses. Total RNA from developing seeds of *T. alata* and *T. laurifolia* were isolated as described above. Developing *Camelina* seeds (10 to 15 d after flowering) were also used RNA isolation with Qiagen Plant Mini kit. DNase I-treated total RNA (1 μg) was used to generate cDNA using RevertAid first-strand cDNA synthesis kit with the oligo dT18 primer (Thermo Scientific). qRT-PCR was performed with the iCycler Real-Time PCR Detection System (Bio-Rad) using the qMax Green qPCR Mix (Benchmark Scientific) in a reaction volume of 20 μL with conditions described previously (59), using *β-TUBULIN* as the internal reference gene. The primers used for qPCR are listed in *SI Appendix*, Table S2. Identical primers were used to measure expression of *T. laurifolia* and *T. alata* genes that were designed from conserved sequences in genes from both species.

Phylogenetic Analyses. Desaturase homologs were collected by using the *T. laurifolia* Δ6-18:0-ACP desaturase protein as the query in a BLASTP search against the National Center for Biotechnology Information protein databank. A smaller dataset (20 sequences) and larger dataset (134 sequences) were aligned using Muscle in MEGA11 (60) and trimmed with Gblocks v0.91b (61). Both alignments were analyzed by maximum likelihood using RAxML v8.2.4 (62) with the PROTGAMMAAUTO model and 1,000 bootstrap replicates.

Protein Modeling. The complex structure of *T. laurifolia* acyl-ACP desaturase and the stearic acid was modeled by using the structure of 18:0-ACP with a docked FA (PDB ID: 2FVA) (63) as a template. All protein structures were visualized by Pymol (The PyMOL Molecular Graphics System, v1.7.X, Schrödinger).

Data Availability. Sequence data for cDNAs described in this study have been deposited in GenBank with the following accession numbers: *TaFATA*: OL757543 (https://www.ncbi.nlm.nih.gov/nuccore/OL757543); *TaFATB1*: OL757544 (https://www.ncbi.nlm.nih.gov/nuccore/OL757544); *TaFATB2*: OL757545 (https://www.ncbi.nlm.nih.gov/nuccore/OL757545); *TaFATB3*: OL757546 (https://www.ncbi.nlm.nih.gov/nuccore/OL757546); *TaKASI*: OL757547 (https://www.ncbi.nlm.nih.gov/nuccore/OL757547); *TaKASII*: OL757548 (https://www.ncbi.nlm.nih.gov/nuccore/OL757548); *TlLPAT2*: OL757549 (https://www.ncbi.nlm.nih.gov/nuccore/OL757549); *TlΔ6-18:0-ACP* desaturase *CDS1*: OL757550 (https://www.ncbi.nlm.nih.gov/nuccore/OL757550); *TlΔ6-18:0-ACP* desaturase *CDS2*: OL757551 (https://www.ncbi.nlm.nih.gov/nuccore/OL757551); *TlΔ9-18:0-ACP* desaturase: ON393910 (https://www.ncbi.nlm.nih.gov/nuccore/ON393910); *TlFATA*: OL757552 (https://www.ncbi.nlm.nih.gov/nuccore/OL757552); *TlFATB1*: OL757553 (https://www.ncbi.nlm.nih.gov/nuccore/OL757553); *TlFATB2*: OL757554 (https://www.ncbi.nlm.nih.gov/nuccore/OL757554); *TlKASI*: OL757555 (https://www.ncbi.nlm.nih.gov/nuccore/OL757555); *TlKASII*: OL757556 (https://www.ncbi.nlm.nih.gov/nuccore/OL757556). Atomic coordinates and structure factor files have been deposited in the RCSB Protein Data Bank, https://doi.org/10.2210/pdb7T63/pdb.

ACKNOWLEDGMENTS. We thank Miles Mayer and Rebecca Cahoon for editing the manuscript; Tara Nazarenus for maintenance of camelina lines; Brian Pfleger and Michael Jindra (University of Wisconsin) for useful discussions about desaturase and thioesterase structure-function; and Joaquín J. Salas (Instituto de la Grasa) and John Ohlrogge (Michigan State University) for providing 1-^{14}C-petroselinoyl-ACP. Research was supported by US Department of Energy (DOE) Center for Advanced Bioenergy and Bioproducts Innovation Award DE- SC0018420 (to J.S. and E.B.C.). Transcriptome sequencing was supported by a NSF Grant Plant Genome IOS-13-39385 (to E.N.M., J.S., and E.B.C.). J.C. and J.S. were supported by the Division of Chemical Sciences, Geosciences, and Biosciences, Office of Basic Energy Sciences, US DOE Award DOE KC0304000. Q.L. was supported by the US DOE, Office of Science, Office of Biological and Environmental Research. The work used National Synchrotron Light source II (NSLS-II), which is supported in part by the US DOE Office of Basic Energy Sciences under Contract DE-SC0012704. Beamline FMX is supported by NIH P30GM133893 and by the DOE Office of Biological and Environmental Research.

Author affiliations: [a]US Department of Energy Center for Advanced Bioenergy and Bioproducts Innovation, University of Nebraska-Lincoln, Lincoln, NE 68588; [b]Center for Plant Science Innovation, University of Nebraska-Lincoln, Lincoln, NE 68588; [c]Department of Biochemistry, University of Nebraska-Lincoln, Lincoln, NE 68588; [d]Department of Biology, Brookhaven National Laboratory, Upton, NY 11973; [e]School of Biological Sciences, University of Nebraska-Lincoln, Lincoln, NE 68588; [f]Department of Computer Science and Engineering, University of Nebraska-Lincoln, Lincoln, NE 68588; [g]Biochemistry & Cell Biology Department, Stony Brook University, Stony Brook, NY 11794; [h]National Key Lab of Crop Genetic Improvement and College of Plant Science and Technology, Huazhong Agricultural University, 430070 Wuhan, China; [i]Department of Agronomy & Horticulture, University of Nebraska-Lincoln, Lincoln, NE 68588; and [j]Department of Pharmacognosy and Pharmaceutical Botany, Excellent Research Laboratory, Phytomedicine and Pharmaceutical Biotechnology Excellence Center, Faculty of Pharmaceutical Sciences, Prince of Songkla University, 91110 Songkla, Thailand

1. R. C. Badami, K. B. Patil, Structure and occurrence of unusual fatty acids in minor seed oils. *Prog. Lipid Res.* **19**, 119–153 (1980).
2. J. Ohlrogge *et al.*, PlantFAdb: A resource for exploring hundreds of plant fatty acid structures synthesized by thousands of plants and their phylogenetic relationships. *Plant J.* **96**, 1299–1308 (2018).
3. C. Smith Jr., Occurrence of unusual fatty acids in plants. *Prog. Chem. Fats Other Lipids* **11**, 137–177 (1971).
4. E. B. Cahoon, Y. Li-Beisson, Plant unusual fatty acids: Learning from the less common. *Curr. Opin. Plant Biol.* **55**, 66–73 (2020).
5. S. Stymne, J. Ohlrogge, Tweaking enzymes for exotic plant oils. *Nat. Plants* **4**, 633–634 (2018).
6. J. Msanne, H. Kim, E. B. Cahoon, Biotechnology tools and applications for development of oilseed crops with healthy vegetable oils. *Biochimie* **178**, 4–14 (2020).
7. S. A. Graham, S. J. Knapp, *Cuphea*: A new plant source of medium-chain fatty acids. *Crit. Rev. Food Sci. Nutr.* **28**, 139–173 (1989).
8. L. Saalmüller, Ueber die fetten Säuren des Ricinusöls. *Justus Liebigs Ann. Chem.* **64**, 108–126 (1848).
9. K. Dehesh, P. Edwards, T. Hayes, A. M. Cranmer, J. Fillatti, Two novel thioesterases are key determinants of the bimodal distribution of acyl chain length of *Cuphea palustris* seed oil. *Plant Physiol.* **110**, 203–210 (1996).
10. K. Dehesh, A. Jones, D. S. Knutzon, T. A. Voelker, Production of high levels of 8:0 and 10:0 fatty acids in transgenic canola by overexpression of *Ch FatB2*, a thioesterase cDNA from *Cuphea hookeriana*. *Plant J.* **9**, 167–172 (1996).
11. F. Jing, L. Zhao, M. D. Yandeau-Nelson, B. J. Nikolau, Two distinct domains contribute to the substrate acyl chain length selectivity of plant acyl-ACP thioesterase. *Nat. Commun.* **9**, 860 (2018).
12. E. B. Cahoon *et al.*, Biosynthetic origin of conjugated double bonds: Production of fatty acid components of high-value drying oils in transgenic soybean embryos. *Proc. Natl. Acad. Sci. U.S.A.* **96**, 12935–12940 (1999).
13. M. Lee *et al.*, Identification of non-heme diiron proteins that catalyze triple bond and epoxy group formation. *Science* **280**, 915–918 (1998).

14. F. J. van de Loo, P. Broun, S. Turner, C. Somerville, An oleate 12-hydroxylase from *Ricinus communis* L. is a fatty acyl desaturase homolog. *Proc. Natl. Acad. Sci. U.S.A.* **92**, 6743–6747 (1995).
15. S. Kazaz, R. Miray, L. Lepiniec, S. Baud, Plant monounsaturated fatty acids: Diversity, biosynthesis, functions and uses. *Prog. Lipid Res.* **85**, 101138 (2022).
16. J. Nagai, K. Bloch, Enzymatic desaturation of stearyl acyl carrier protein. *J. Biol. Chem.* **241**, 1925–1927 (1966).
17. J. E. Guy, E. Whittle, D. Kumaran, Y. Lindqvist, J. Shanklin, The crystal structure of the ivy Δ^4-16:0-ACP desaturase reveals structural details of the oxidized active site and potential determinants of regioselectivity. *J. Biol. Chem.* **282**, 19863–19871 (2007).
18. Y. Lindqvist, W. Huang, G. Schneider, J. Shanklin, Crystal structure of Δ^9 stearoyl-acyl carrier protein desaturase from castor seed and its relationship to other di-iron proteins. *EMBO J.* **15**, 4081–4092 (1996).
19. E. B. Cahoon, Y. Lindqvist, G. Schneider, J. Shanklin, Redesign of soluble fatty acid desaturases from plants for altered substrate specificity and double bond position. *Proc. Natl. Acad. Sci. U.S.A.* **94**, 4872–4877 (1997).
20. H. T. Nguyen *et al.*, Redirection of metabolic flux for high levels of omega-7 monounsaturated fatty acid accumulation in camelina seeds. *Plant Biotechnol. J.* **13**, 38–50 (2015).
21. E. B. Cahoon, J. B. Ohlrogge, Metabolic evidence for the involvement of a Δ^4-palmitoyl-acyl carrier protein desaturase in petroselinic acid synthesis in coriander endosperm and transgenic tobacco cells. *Plant Physiol.* **104**, 827–837 (1994).
22. E. B. Cahoon, J. Shanklin, J. B. Ohlrogge, Expression of a coriander desaturase results in petroselinic acid production in transgenic tobacco. *Proc. Natl. Acad. Sci. U.S.A.* **89**, 11184–11188 (1992).
23. S. Mekhedov, E. B. Cahoon, J. Ohlrogge, An unusual seed-specific 3-ketoacyl-ACP synthase associated with the biosynthesis of petroselinic acid in coriander. *Plant Mol. Biol.* **47**, 507–518 (2001).
24. M. C. Suh, D. J. Schultz, J. B. Ohlrogge, What limits production of unusual monoenoic fatty acids in transgenic plants? *Planta* **215**, 584–595 (2002).
25. E. B. Cahoon, A. M. Cranmer, J. Shanklin, J. B. Ohlrogge, Δ^6 Hexadecenoic acid is synthesized by the activity of a soluble Δ^6 palmitoyl-acyl carrier protein desaturase in *Thunbergia alata* endosperm. *J. Biol. Chem.* **269**, 27519–27526 (1994).
26. G. F. Spencer, R. Kleiman, R. W. Miller, F. R. Earle, Occurrence of *cis*-6-hexadecenoic acid as the major component of *Thunbergia alata* seed oil. *Lipids* **6**, 712–714 (1971).
27. E. B. Cahoon, C. K. Becker, J. Shanklin, J. B. Ohlrogge, cDNAs for isoforms of the Δ^9-stearoyl-acyl carrier protein desaturase from *Thunbergia alata* endosperm. *Plant Physiol.* **106**, 807–808 (1994).
28. E. Whittle, E. B. Cahoon, S. Subrahmanyam, J. Shanklin, A multifunctional acyl-acyl carrier protein desaturase from *Hedera helix* L. (English ivy) can synthesize 16- and 18-carbon monoene and diene products. *J. Biol. Chem.* **280**, 28169–28176 (2005).
29. E. Whittle, J. Shanklin, Engineering Δ^9-16:0-acyl carrier protein (ACP) desaturase specificity based on combinatorial saturation mutagenesis and logical redesign of the castor Δ^9-18:0-ACP desaturase. *J. Biol. Chem.* **276**, 21500–21505 (2001).
30. H. T. Nguyen *et al.*, Camelina seed transcriptome: A tool for meal and oil improvement and translational research. *Plant Biotechnol. J.* **11**, 759–769 (2013).
31. P. Dormann, M. Frentzen, J. B. Ohlrogge, Specificities of the acyl-acyl carrier protein (ACP) thioesterase and glycerol-3-phosphate acyltransferase for octadecenoyl-ACP Isomers (identification of a petroselinoyl-ACP thioesterase in Umbelliferae). *Plant Physiol.* **104**, 839–844 (1994).
32. K. T. Achaya, B. M. Craig, C. G. Youngs, The component fatty acids and glycerides of castor oil. *J. Am. Oil Chem. Soc.* **41**, 783–784 (1964).
33. J. Fernández-Martinez, M. del Rio, A. de Haro, Survey of safflower (*Carthamus tinctorius* L.) germplasm for variants in fatty acid composition and other seed characters. *Euphytica* **69**, 115–122 (1993).
34. J. E. Guy *et al.*, Regioselectivity mechanism of the *Thunbergia alata* Δ^6-16:0-acyl carrier protein desaturase. *Plant Physiol.* **188**, 1537–1549 (2022).
35. J. B. Ohlrogge, Design of new plant products: Engineering of fatty acid metabolism. *Plant Physiol.* **104**, 821–826 (1994).
36. L. L. Placek, A review on petroselinic acid and its derivatives. *J. Am. Oil Chem. Soc.* **40**, 319–329 (1963).
37. W. H. Heimermann, R. T. Holman, D. T. Gordon, D. E. Kowalyshyn, R. G. Jensen, Effect of double bond position in octadecenoates upon hydrolysis by pancreatic lipase. *Lipids* **8**, 45–47 (1973).
38. E. G. Bligh, W. J. Dyer, A rapid method of total lipid extraction and purification. *Can. J. Biochem. Physiol.* **37**, 911–917 (1959).
39. R. L. Wolff, C. C. Bayard, R. J. Fabien, Evaluation of sequential methods for the determination of butterfat fatty acid composition with emphasis on *trans*-18:1 acids. Application to the study of seasonal variations in French butters. *J. Am. Oil Chem. Soc.* **72**, 1471–1483 (1995).
40. E. B. Cahoon, J. B. Ohlrogge, Apparent role of phosphatidylcholine in the metabolism of petroselinic acid in developing Umbelliferae endosperm. *Plant Physiol.* **104**, 845–855 (1994).
41. E. B. Cahoon *et al.*, Conjugated fatty acids accumulate to high levels in phospholipids of metabolically engineered soybean and *Arabidopsis* seeds. *Phytochemistry* **67**, 1166–1176 (2006).
42. X. Li *et al.*, Discontinuous fatty acid elongation yields hydroxylated seed oil with improved function. *Nat. Plants* **4**, 711–720 (2018).
43. D. L. Wheeler *et al.*, Database resources of the National Center for Biotechnology. *Nucleic Acids Res.* **31**, 28–33 (2003).
44. C. Camacho *et al.*, BLAST+: Architecture and applications. *BMC Bioinformatics* **10**, 421 (2009).
45. C. Y. Cheng *et al.*, Araport11: A complete reannotation of the *Arabidopsis thaliana* reference genome. *Plant J.* **89**, 789–804 (2017).
46. A. Priyam *et al.*, Sequenceserver: A modern graphical user interface for custom BLAST databases. *Mol. Biol. Evol.* **36**, 2922–2924 (2019).
47. C. Lu, J. Kang, Generation of transgenic plants of a potential oilseed crop *Camelina sativa* by Agrobacterium-mediated transformation. *Plant Cell Rep.* **27**, 273–278 (2008).
48. D. K. Schneider *et al.*, FMX–The frontier microfocusing macromolecular crystallography beamline at the National Synchrotron Light Source II. *J. Synchrotron Radiat.* **28**, 650–665 (2021).
49. D. G. Waterman *et al.*, Diffraction-geometry refinement in the DIALS framework. *Acta Crystallogr. D Struct. Biol.* **72**, 558–575 (2016).
50. G. Evans, D. Axford, D. Waterman, R. L. Owen, Macromolecular microcrystallography. *Crystallogr. Rev.* **17**, 105–142 (2011).
51. P. R. Evans, G. N. Murshudov, How good are my data and what is the resolution? *Acta Crystallogr. D Biol. Crystallogr.* **69**, 1204–1214 (2013).
52. A. J. McCoy *et al.*, Phaser crystallographic software. *J. Appl. Crystallogr.* **40**, 658–674 (2007).
53. P. Emsley, B. Lohkamp, W. G. Scott, K. Cowtan, Features and development of Coot. *Acta Crystallogr. D Biol. Crystallogr.* **66**, 486–501 (2010).
54. P. V. Afonine *et al.*, Towards automated crystallographic structure refinement with phenix.refine. *Acta Crystallogr. D Biol. Crystallogr.* **68**, 352–367 (2012).
55. N. Echols *et al.*, Automated identification of elemental ions in macromolecular crystal structures. *Acta Crystallogr. D Biol. Crystallogr.* **70**, 1104–1114 (2014).
56. R. Laskowski, M. W. Macarthur, D. S. Moss, J. Thornton, PROCHECK: A program to check the stereochemical quality of protein structures. *J. Appl. Crystallogr.* **26**, 283–291 (1993).
57. V. B. Chen *et al.*, MolProbity: All-atom structure validation for macromolecular crystallography. *Acta Crystallogr. D Biol. Crystallogr.* **66**, 12–21 (2010).
58. E. B. Cahoon, J. Shanklin, Substrate-dependent mutant complementation to select fatty acid desaturase variants for metabolic engineering of plant seed oils. *Proc. Natl. Acad. Sci. U.S.A.* **97**, 12350–12355 (2000).
59. A. Gonzalez-Solis *et al.*, Unregulated sphingolipid biosynthesis in gene-edited *Arabidopsis ORM* mutants results in nonviable seeds with strongly reduced oil content. *Plant Cell* **32**, 2474–2490 (2020).
60. K. Tamura, G. Stecher, S. Kumar, MEGA11: Molecular evolutionary genetics analysis version 11. *Mol. Biol. Evol.* **38**, 3022–3027 (2021).
61. J. Castresana, Selection of conserved blocks from multiple alignments for their use in phylogenetic analysis. *Mol. Biol. Evol.* **17**, 540–552 (2000).
62. A. Stamatakis, RAxML version 8: A tool for phylogenetic analysis and post-analysis of large phylogenies. *Bioinformatics* **30**, 1312–1313 (2014).
63. G. A. Zornetzer, B. G. Fox, J. L. Markley, Solution structures of spinach acyl carrier protein with decanoate and stearate. *Biochemistry* **45**, 5217–5227 (2006).